Highly improved passivation of c-Si surfaces using a gradient i a-Si:H layer

Soonil Lee, Jaehyun Ahn, Leo Mathew, Rajesh Rao, Zhongjian Zhang, Jae Hyun Kim, Sanjay K. Banerjee, and Edward T. Yu

Citation: Journal of Applied Physics **123**, 163101 (2018); doi: 10.1063/1.5023000
View online: https://doi.org/10.1063/1.5023000
View Table of Contents: http://aip.scitation.org/toc/jap/123/16
Published by the American Institute of Physics

Highly improved passivation of c-Si surfaces using a gradient *i* a-Si:H layer

Soonil Lee,[1] Jaehyun Ahn,[1] Leo Mathew,[2] Rajesh Rao,[2] Zhongjian Zhang,[1] Jae Hyun Kim,[1] Sanjay K. Banerjee,[1] and Edward T. Yu[1,a)]
[1]*Microelectronics Research Center, The University of Texas at Austin, 10100 Burnet Rd., Building 160, Austin, Texas 78758, USA*
[2]*Applied Novel Devices, Inc., 10100 Burnet Rd., Building 160, Austin, Texas 78758, USA*

(Received 19 January 2018; accepted 10 April 2018; published online 26 April 2018)

Surface passivation using intrinsic a-Si:H (*i* a-Si:H) films plays a key role in high efficiency c-Si heterojunction solar cells. In this study, we demonstrate improved passivation quality using *i* a-Si:H films with a gradient-layered structure consisting of interfacial, transition, and capping layers deposited on c-Si surfaces. The H_2 dilution ratio (R) during deposition was optimized individually for the interfacial and capping layers, which were separated by a transition layer for which R changed gradually between its values for the interfacial and capping layers. This approach yielded a significant reduction in surface carrier recombination, resulting in improvement of the minority carrier lifetime from 1480 μs for mono-layered *i* a-Si:H passivation to 2550 μs for the gradient-layered passivation approach. *Published by AIP Publishing.*
https://doi.org/10.1063/1.5023000

I. INTRODUCTION

Silicon heterojunction (SHJ) solar cells have attracted substantial interest for high-efficiency photovoltaic energy harvesting. Typically, SHJ solar cells have been fabricated by combining c-Si substrates and a-Si:H films in device structures such as interdigitated back contact (IBC),[1,2] and heterostructure with intrinsic thin layer (HIT)[3,4] solar cells. In SHJ solar cells, a key factor for high efficiency is suppressing carrier recombination at the a-Si:H/c-Si interface since it affects the minority carrier lifetime and open circuit voltage (*V*oc). To reduce recombination rates, the c-Si surface can be passivated by thermal annealing treatments,[5] H_2 plasma treatment,[6,7] or thin film deposition.[8] Among the various treatments, surface passivation using intrinsic a-Si:H (*i* a-Si:H) thin films has been very effective due to passivation of Si dangling bonds at the *i* a-Si:H/c-Si interface.[9]

Typically, *i* a-Si:H passivation layers have been deposited using chemical vapor deposition (CVD)-based methods such as plasma-enhanced CVD (PECVD),[10–13] hot wire CVD (HWCVD),[14] and electron cyclotron resonance CVD (ECR-CVD).[15] In *i* a-Si:H CVD processes, the passivation quality is mainly affected by H_2 dilution ratio (R), i.e., the ratio between H_2 and SiH_4 gas flow rates ($R = [H_2]/[SiH_4]$), since R influences crystallinity, defect density, and hydrogen content of the *i* a-Si:H film.[12,16] Many studies have demonstrated good passivation quality using *i* a-Si:H layers deposited with optimized R values during the CVD process.[16–18] In 2014, Lee *et al.*[16] reported on the improved passivation of c-Si surfaces using dual-layered *i* a-Si:H thin films which were deposited with different R values. These dual-layered *i* a-Si:H films consisted of a bottom interfacial layer with optimized R for reducing defects at the c-Si surface, and a top capping layer with high R for reducing micro-voids within the *i* a-Si:H film. This dual-layered passivation approach yielded a 33.4% improvement in the minority carrier lifetime compared to a mono-layered *i* a-Si:H film.

Herein, we demonstrate and characterize improvements in passivation of c-Si surfaces using 10 nm gradient-layered *i* a-Si:H films deposited by remote plasma enhanced CVD (RPCVD), and demonstrate improved efficiency of a SHJ solar cell employing this passivation approach. The gradient-layered *i* a-Si:H films consisted of interfacial, transition, and capping layers which were deposited by RPCVD with a varying H_2 to SiH_4 dilution ratio, R, during deposition. R values for the interfacial and capping layers were optimized by comparing 10 nm mono- and dual-layered *i* a-Si:H films fabricated with different R values. The transition layer was deposited with R increasing gradually between the interfacial and capping layer values to achieve a gradual rather than abrupt transition between these layers. The design of the gradient-layered passivation structure was optimized by varying the thicknesses of the interfacial and transition layers while keeping the total thickness of the *i* a-Si:H films fixed at 10 nm. The improvement in passivation quality for gradient-layered *i* a-Si:H films was evaluated by measuring minority carrier lifetime and analyzing photoluminescence (PL) mapping images and surface recombination velocity (SRV) compared to mono- and dual-layered passivation films.

II. EXPERIMENTAL

As-cut n-type (100) c-Si wafers (thickness $t \sim 180\ \mu$m and resistivity $\rho \sim 2.0\ \Omega$ cm) of commercial solar grade for mass production were cut into 5 cm × 5 cm samples and cleaned with standard RCA solutions. To reduce the surface defect density, a saw damage removal (SDR) process was used. In this process, as-cut c-Si substrates were etched in 20% KOH aqueous solution at 70 °C for 40 min until a

a)Author to whom correspondence should be addressed: ety@ece.utexas.edu. Present address: Electrical and Computer Engineering, The University of Texas at Austin, 10100 Burnet Road, Austin, Texas 78758, USA.

TABLE I. Process parameters for the deposition of intrinsic a-Si:H layers using RPCVD.

H_2 dilution ratio ($R = [H_2]/[SiH_4]$)	Gas flows (sccm)			Plasma Power (W)	Pressure (mTorr)	Temperature (°C)	Deposition rate (nm/min)
	Ar	H_2	SiH_4				
0	100	0	5	30	515	250	0.77
2.5	100	12.5	5	30	522	250	0.74
5	100	25	5	30	530	250	0.71
7	100	35	5	30	537	250	0.66
9	100	45	5	30	544	250	0.54
11	100	55	5	30	550	250	0.46
13	100	65	5	30	556	250	0.42

thickness of 150 μm was reached. The etched c-Si substrates were then dipped in an $HCl:H_2O_2:H_2O$ 5:1:1 solution to remove K^+ ions from the c-Si surface. *i* a-Si:H films were deposited by RPCVD on both sides of the SDR processed c-Si substrates with *i* a-Si:H/c-Si/*i* a-Si:H (*i*/c-Si/*i*) structure. During the deposition process, the processing temperature and plasma power were maintained at 250 °C and 30 W, respectively. The process gas flows for Ar, SiH_4, and H_2 were controlled by a mass flow controller (MFC) system with varying R as presented in Table I. All the *i* a-Si:H passivation films were deposited with 10 nm total thickness based on prior reports that 5–10 nm *i* a-Si:H films showed very good passivation quality on c-Si substrates without electrical and optical losses.[2,19] To evaluate the effect of these layers on surface passivation for SHJ solar cell structures, 10 nm n-type and p-type a-Si:H layers were deposited by RPCVD on both sides, after passivating 150 μm thick SDR processed c-Si substrates with mono-, dual-, and gradient-layered passivation schemes. Detailed deposition parameters for each a-Si:H layer are presented in Table II.

To calibrate *i* a-Si:H deposition rates and film thicknesses, *i* a-Si:H films were deposited on Si/SiO_2 wafers (SiO_2 thickness $t \sim 200$ nm), and the *i* a-Si:H layer thicknesses were then measured using spectroscopic ellipsometry. For Raman measurements, 10 nm *i* a-Si:H films were deposited on slide glass with R values ranging from 0 to 12.5. Raman spectra for *i* a-Si:H films were measured with a 532 nm laser source using a commercial Raman spectroscopy system (Renishaw 2000) before and after annealing at 300 °C for 30 min. Fourier transform infrared (FT-IR) measurements were performed for 10 nm *i* a-Si:H films on c-Si substrates which were deposited with R values ranging from 0 to 12.5 using a commercial FT-IR spectrometer (Nicolet-iS50R). The passivation quality of the *i* a-Si:H films was evaluated by measuring the minority carrier lifetimes and using photoluminescence (PL) mapping of passivated c-Si wafers. The effective minority carrier lifetimes of SDR processed c-Si substrates which were passivated with different *i* a-Si:H passivation schemes were measured by the photoconductance decay method using a Sinton lifetime tester (WCT 120). For PL mapping images, SDR processed c-Si substrates were passivated by 10 nm *i* a-Si:H films with mono-, dual-, and gradient-layered passivation schemes. PL signals were measured with a 532 nm laser source using a commercial Raman spectroscopy system (Renishaw 2000).

III. RESULTS AND DISCUSSION

Figure 1(a) shows the normalized FT-IR absorption spectra for 10 nm *i* a-Si:H films on c-Si substrates deposited by RPCVD with R ranging from 0 to 12.5. In the region from 1900 to 2200 cm^{-1}, the Si-H and $Si-H_2$ stretching bond peaks are clearly visible near 2010 cm^{-1} and 2080 cm^{-1}, respectively.[18] It has been reported that, during *i* a-Si:H deposition using RPCVD, H_2 gas suppresses the formation of $Si-H_2$ bonds leading to a high density of micro-voids and defects.[17] The *i* a-Si:H film with the lowest hydrogen dilution ($R = 0$) showed the highest intensity in Si-H and $Si-H_2$ stretching bonds. As R increased from 0 to 12.5, a progressive decrease in the Si-H stretching bond peak at 2010 cm^{-1} was observed. For the $Si-H_2$ stretching bond peak at 2080 cm^{-1}, the peak intensity dramatically decreased as R increased from 0 to 5, and then moderately decreased as R increased further, from 5 to 12.5. From these observations, we conclude that the RPCVD process with high R leads to a low H content and low densities of Si-H and $Si-H_2$ stretching bonds, thereby reducing the concentration of micro-voids and defects in *i* a-Si:H film.

Conversely, it has been reported that high R values in *i* a-Si:H deposition cause epitaxial growth and the formation

TABLE II. Process parameters for the a-Si:H passivation with doping layers using RPCVD.

Layer	Gas flows (sccm)					Plasma Power (W)	Pressure (mTorr)	Temperature (°C)
	Ar	H_2	SiH_4	PH_3	B_2H_6			
Mono-layered *i* a-Si:H	100	25	5	…	…	30	530	250
Dual-layered *i* a-Si:H	100	25/65	5	…	…	30	530/556	250
Gradient-layered *i* a-Si:H	100	25∼65	5	…	…	30	530∼556	250
n-type a-Si:H	100	25	5	100	…	30	600	250
p-type a-Si:H	100	25	5	…	100	30	600	250

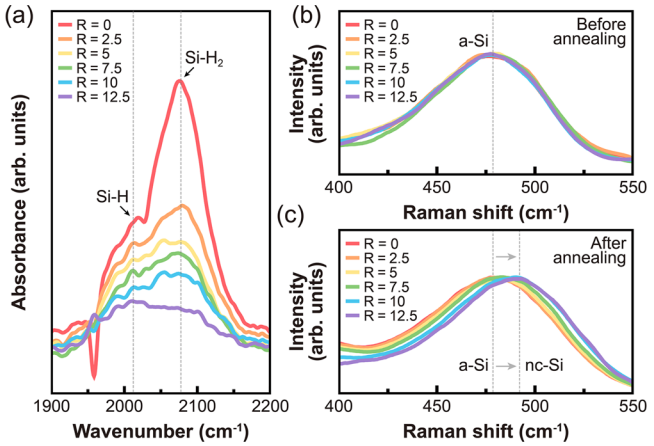

FIG. 1. (a) Normalized FT-IR spectra for 10 nm *i* a-Si:H films on c-Si substrates deposited by RPCVD with different R values. (b) and (c) Normalized Raman spectra for 10 nm *i* a-Si:H films on glass substrates deposited by RPCVD with different R values, (b) before and (c) after annealing at 300 °C for 30 min.

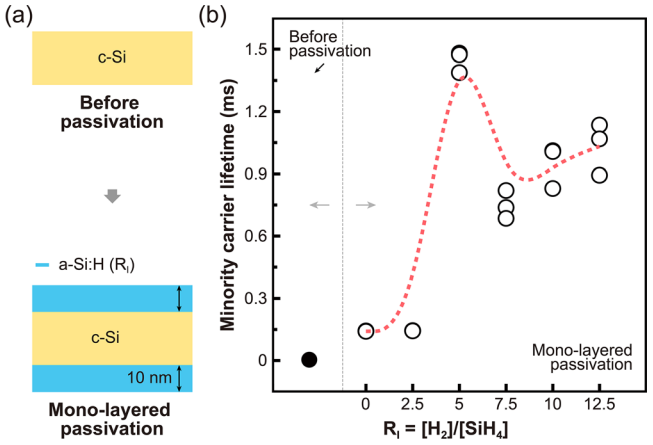

FIG. 2. (a) Schematic of the fabrication process of mono-layered passivation on the c-Si substrate. (b) The effective minority carrier lifetime of the c-Si substrate before passivation (Black filled circles) and after passivation using 10 nm mono-layered *i* a-Si:H films (Black hollow circles) as a function of R_I. The red-dotted line plots the trend of measured minority carrier lifetimes.

of nano-crystalline Si (nc-Si) at the *i* a-Si:H/c-Si interface.[20] Figures 1(b) and 1(c) show the normalized Raman spectra for 10 nm *i* a-Si:H films on glass substrates before and after an annealing at 300 °C for R ranging from 0 to 12.5. Typically, Si peaks are observed from 350 to 550 cm^{-1}, and peaks associated specifically with a-Si and c-Si are positioned near 480 cm^{-1} and 510 cm^{-1}, respectively.[21] The pre-phase nucleation of nc-Si leads to a minor red-shift of the a-Si peak at 480 cm^{-1} in the Raman spectra.[22,23] As shown in Fig. 1(b), strong a-Si peaks were observed at 480 cm^{-1} in *i* a-Si:H films for all R values. However, after annealing at 300 °C for 30 min, shifts of the a-Si peaks to 490 cm^{-1} were clearly observed. Under atmospheric pressure, phase transitions from a-Si to nc-Si occur at temperatures above 300 °C.[24] As shown in Fig. 1(c), shifts of the a-Si peaks caused by this phase transition become more obvious as R values are increased. The red shift observed in the Raman spectra with higher R suggests that small pre-phase seeds of nc-Si were grown in *i* a-Si:H films deposited with high R. Since these epitaxial seeds act as additional recombination centers at the *i* a-Si:H/c-Si interface, values of R that are too high can lead to poor passivation quality.

In the *i* a-Si:H passivation scheme, the interfacial layer deposited on the c-Si surface serves to passivate dangling bonds at the *i* a-Si:H/c-Si interface. To obtain optimal passivation quality at this interfacial layer, optimizing R is crucial since too low R causes more micro-voids and defects in the *i* a-Si:H film and too high R causes epitaxial growth at the *i* a-Si:H/c-Si interface. As shown in Fig. 2(a), we first characterized samples for which both sides of the c-Si substrates were passivated by 10 nm mono-layered *i* a-Si:H films with varying R values for the interfacial layer (R_I). Figure 2(b) shows the measured minority carrier lifetime for c-Si substrates with mono-layered passivation at a 1×10^{15} cm^{-3} injection level as a function of R_I. The measurement of minority carrier lifetime using the quasi-steady-state photoconductance (QSSPC) method is used as a measure of the passivation quality of different *i* a-Si:H films. Before passivation, the minority carrier lifetime of the bare c-Si substrate was <15 μs. For R_I below 2.5, the c-Si substrate with mono-layered passivation showed poor passivation quality, with a minority carrier lifetime of $\sim$150 μs. This poor passivation at low R_I was attributed to the high density of micro-voids and defects in *i* a-Si:H film, as indicated by the high intensity of Si-H$_2$ stretching bonds shown in Fig. 1(a) for low values of R. At $R_I = 5$, the minority carrier lifetime of the passivated c-Si substrate increased dramatically, to $\sim$1400 μs. The minority carrier lifetime then dropped substantially, to $\sim$800 μs, at $R_I = 7.5$, then increased slowly with increasing R_I, reaching $\sim$1000 μs at $R_I = 12.5$. We attribute this sharp reduction in the minority carrier lifetime between $R = 5$ and $R = 7.5$ to the increased presence of nc-Si at the *i* a-Si:H/c-Si interface, as indicated by the Raman spectra in Figs. 1(b) and 1(c). As a result, the mono-layered passivation using *i* a-Si:H film with $R_I = 5$ was deemed to be optimal, with a minority carrier lifetime up to 1480 μs at a 1×10^{15} cm^{-3} injection level.

It has been reported that dual-layered *i* a-Si:H films which contain an additional capping layer atop the interfacial layer, with the R value of the capping layer (R_C) higher than R_I, yield improved passivation quality compared to mono-layered passivation.[16] This is possible because for *i* a-Si:H deposition on an a-Si:H substrate, epitaxial growth occurs at a higher R value compared to that for deposition on a c-Si substrate.[12] Therefore, deposition of a capping layer with high R_C can yield a lower density of micro-voids and defects in an entire dual-layered *i* a-Si:H film without degradation caused by epitaxial growth.

To determine optimal values of R_C for dual-layered *i* a-Si:H passivation structures, c-Si substrates were passivated with 10 nm dual-layered *i* a-Si:H films consisting of a 5 nm interfacial *i* a-Si:H layer deposited on the c-Si substrate with optimized $R_I = 5$, followed by 5 nm capping *i* a-Si:H layers with different R_C values, as shown in Fig. 3(a). Figure 3(b) shows the measured minority carrier lifetimes of c-Si substrates passivated by these dual-layered *i* a-Si:H films at 1×10^{15} cm^{-3} injection level, as a function of R_C. Every

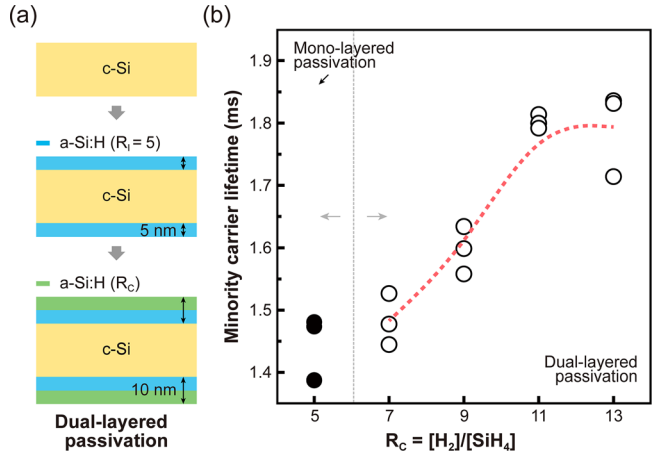

FIG. 3. (a) Schematic of the fabrication process of dual-layered passivation on c-Si the substrate. (b) The effective minority carrier lifetime of the c-Si substrate passivated using 10 nm mono-layered (Black filled circles) and dual-layered (Black hollow circles) *i* a-Si:H films as a function of R_C value. The red-dotted line plots the trend of measured minority carrier lifetimes.

dual-layered *i* a-Si:H film with R_C above 5 showed higher minority carrier lifetime than optimized mono-layered *i* a-Si:H films with $R_I = 5$. As R_C increased, the minority carrier lifetime moderately increased, leveling off for $R_C = 13$ at ~1800 μs. As a result, the dual-layered passivation using *i* a-Si:H films with $R_I = 5$ and $R_C = 13$ showed the best performance, with minority carrier lifetime up to 1830 μs at 1×10^{15} cm^{-3} injection level.

In the dual-layered *i* a-Si:H films, there is an abrupt transition between the interfacial and capping layers. The abrupt interface can cause carrier trapping in the heterojunction due to recombination centers formed at the interface[25] combined with minority carrier accumulation due to the valence-band offset between c-Si and a-Si:H.[26] To reduce the carrier recombination caused by the abrupt interface in dual-layered passivation, we fabricated gradient-layered *i* a-Si:H films in which the abrupt interface was replaced by one in which R was changed gradually. As shown in Fig. 4(a), the gradient-layered passivation consists of interfacial, transition, and capping layers. The interfacial and capping layers were deposited with optimized R_I and R_C values of 5 and 13, respectively. For the transition layer, R (R_T) was ramped linearly across the transition layer from 5 to 13 by controlling the H_2 flow during RPCVD deposition to create a graded interface between the interfacial and capping layers.

To investigate the relationship between passivation quality and design parameters in gradient-layered passivation, c-Si substrates were passivated by gradient-layered *i* a-Si:H films with different designs and their minority carrier lifetimes were measured. At first, R_T was varied by varying the thickness of the transition layer (t_T). Figure 4(b) shows a schematic representation of R during *i* a-Si:H deposition as a function of the film thickness for different values of t_T. 3 gradient-layered passivation structures (designated Gradient 1, 2, and 3) were designed with different t_T. For these designs, R_T was increased from 5 to 13 across transition layers 4 nm, 6 nm, and 8 nm in thickness for Gradient 1, 2, and 3, respectively. Figure 4(c) shows the measured minority carrier lifetimes of c-Si substrates passivated on both sides by 10 nm gradient-layered *i* a-Si:H films with Gradient 1, 2, or 3. Compared to dual-layered passivation, gradient-layered passivation with any design showed higher minority carrier lifetime. As t_T increased, R_T changed more gradually during deposition of the transition layer and the minority carrier lifetime of the c-Si substrate with gradient-layered passivation was improved. The c-Si substrate passivated by a 10 nm gradient-layered *i* a-Si:H film with the Gradient 3 design showed the best passivation quality, with a minority carrier lifetime of 2550 μs. Thus, changing R_T gradually during deposition of the transition layer enhances the passivation quality of gradient-layered *i* a-Si:H films, with a more gradual change in R_T leading to higher passivation quality.

Interfacial layer thickness can also influence passivation quality, with too thin an interfacial layer causing passivation quality to degrade. In particular, it has been reported that the thickness of the interfacial layer (t_I) can significantly affect fixed charges at the a-Si:H/c-Si interface.[27] To confirm the relationship between passivation quality and the thickness of the interfacial layer in gradient-layered *i* a-Si:H films, three additional structures, designated Gradient 4, 5, and 6, were designed with fixed t_T and different t_I of 1 nm, 2 nm, and 3 nm, respectively, as shown in Fig. 4(d). Figure 4(e) shows the measured minority carrier lifetime of c-Si substrates passivated with structures corresponding to Gradient 4, 5, and 6 at 1×10^{15} cm^{-3} injection level. Compared to dual-layered passivation, gradient-layered passivation with Gradient 4, 5, and 6 designs also showed improved passivation quality. When t_I increased from 1 nm to 2 nm, the minority carrier lifetime increased as well. However, when t_I was above 2 nm, c-Si substrates passivated with both Gradient 5 and 6 showed similar minority carrier lifetimes of ~2100 μs. This result indicates that the thickness of interfacial layer should be at least 2 nm for the effective reduction of fixed charges at the a-Si:H/c-Si interface. Similarly, in the case of dual-layered passivation, the passivation quality might also increase with increasing t_I and saturate beyond a thickness between 2 and 5 nm. The saturated minority carrier lifetime of c-Si substrate passivated by dual-layered *i* a-Si:H films is likely to be similar with the case of dual-layered passivation consisting of 5 nm t_I.

For the passivation of c-Si using *i* a-Si:H films, not only the film quality but also the uniformity of the deposited *i* a-Si:H film is an important factor to evaluate passivation quality. To evaluate the uniformity of passivation layers, PL mapping images were measured on the surfaces of c-Si substrates before and after surface passivation. Figure 5 shows measured PL mapping images on 3 cm × 3 cm SDR processed c-Si substrates before and after passivation using mono-, dual-, and gradient-layered *i* a-Si:H films. The uniformity of PL mapping image can be referred by calculating a relative standard deviation (RSD) of PL signals as follows:

$$RSD = \frac{\sigma}{\mu} \times 100\%, \tag{1}$$

where σ is the standard deviation and μ is the mean of PL measured signals. Before passivation, significant

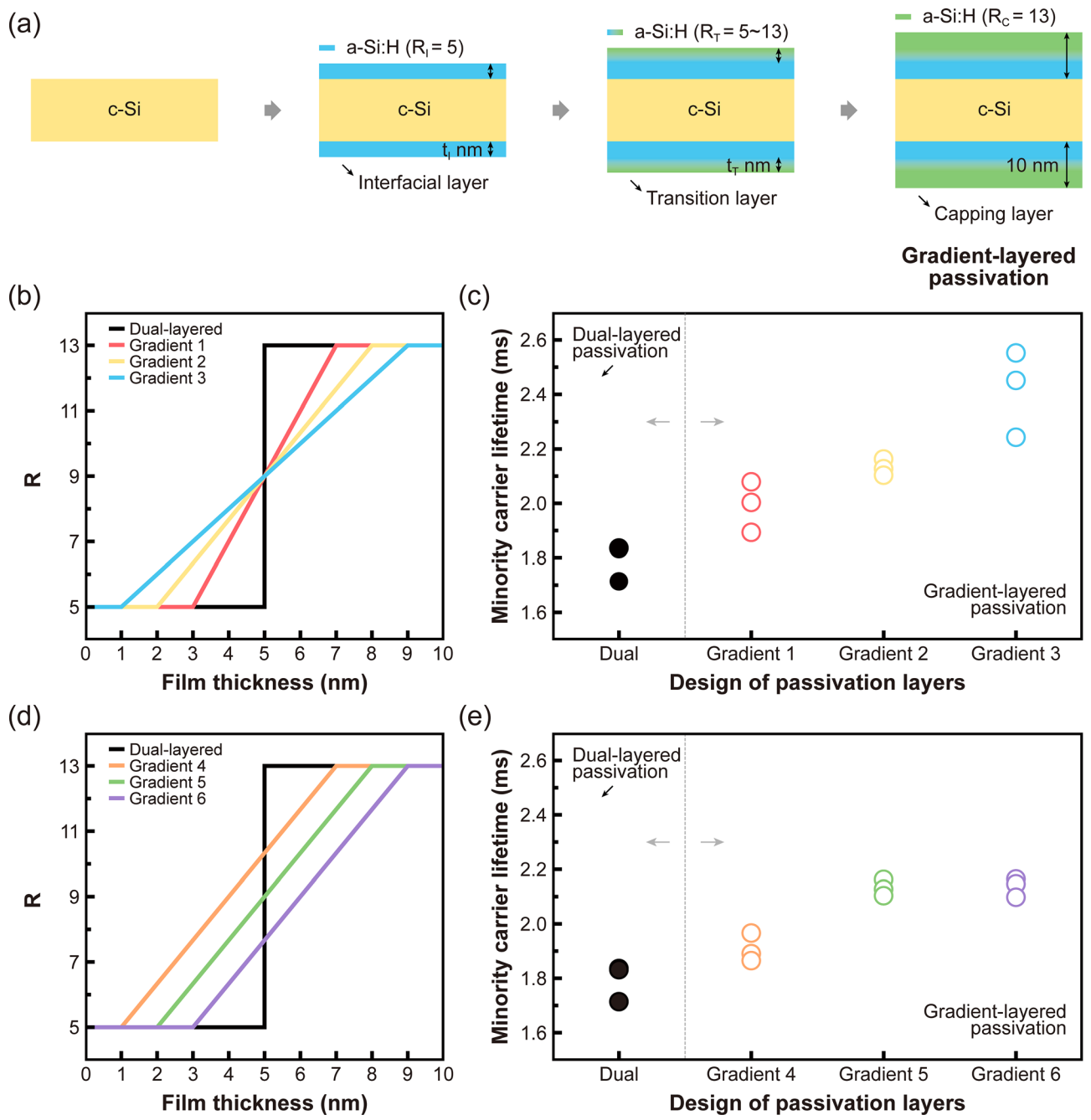

FIG. 4. (a) Schematic of the fabrication process of gradient-layered passivation on the c-Si substrate. (b) and (d) Schematic representation off changes of the R value during the deposition for different designs of *i* a-Si:H passivation layers as a function of film thickness. (c) and (e) The effective minority carrier lifetime of the c-Si substrate passivated by 10 nm *i* a-Si:H films for different designs of passivation layers.

nonuniformity was observed on the c-Si surface with a relative standard deviation (RSD) of 19.98%. It is known that such nonuniformities can arise from surface defects on the c-Si substrate, with recombination at these sites leading to low minority carrier lifetimes.[28] Compared to the non-passivated c-Si substrate, much more uniform PL images were observed in every passivated c-Si substrate with mono-, dual-, and gradient-layered *i* a-Si:H passivation films, with all passivation structures showing similar levels of uniformity with a low RSD of around 9.00%. Since each passivation method showed similar uniformity, we conclude that the different results in passivation quality of *i* a-Si:H films as determined from minority carrier lifetime measurements were influenced primarily by the passivation scheme rather than nonuniformity.

In *i* a-Si:H passivation of c-Si surfaces, the passivation quality can be influenced by numerous factors including dangling bonds on the c-Si surface and defect centers in the *i* a-Si:H film. The effective surface recombination velocity (S_{eff}) of the c-Si substrate can be used to directly quantify the passivation quality of the *i* a-Si:H film. S_{eff} can be estimated from the measured effective minority carrier lifetime (τ_{eff}) using the following simplified equation:[29]

$$S_{\text{eff}} = \left(\frac{1}{\tau_{\text{eff}}} - \frac{1}{\tau_{\text{bulk}}}\right)\frac{d_{\text{Si}}}{2}, \tag{2}$$

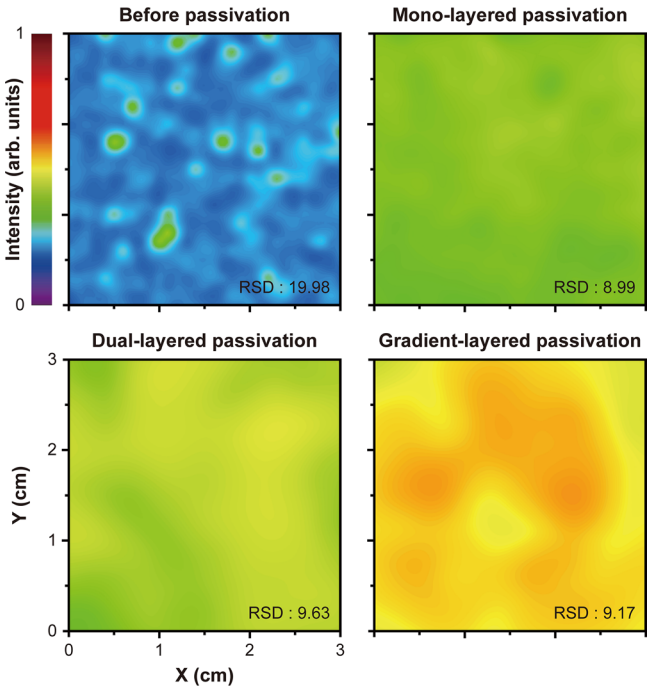

FIG. 5. PL mapping images for 3 cm × 3 cm c-Si substrates before and after mono-, dual-, and gradient-layered passivation using 10 nm *i* a-Si:H films. The RSD values of each PL image are inside of PL mapping images, individually.

where τ_{bulk} is the bulk Shockley-Reed-Hall lifetime and d_{Si} is the thickness of the c-Si substrate. It was assumed that τ_{bulk} did not change during a-Si:H deposition, annealing at 300 °C, or measurement of τ_{eff}. We set τ_{bulk} to a typical value of 10 ms,[29] and the c-Si substrate was 150 μm in thickness. Before passivation, the calculated S_{eff} was very high (500 cm s^{-1}) since there are many defect sites at the surface of the c-Si substrate. Figure 6(a) shows a plot of S_{eff} calculated from Eq. (2) as a function of τ_{eff} for c-Si substrate passivated by mono-, dual-, and gradient-layered *i* a-Si:H films. The SRV and the density of surface recombination centers on the c-Si surface can be modeled as a linear relationship as follows:[30]

$$S_{eff} = \sigma v_{th} N_t , \quad (3)$$

where σ is the recombination cross section, v_{th} is the carrier thermal velocity, and N_t is the number of recombination centers per square centimeter. Typical values for σ and v_{th} are 10^{-16} cm^2 and 10^7 cm s^{-1}, respectively.[31] Based on Eqs. (2) and (3), the density of recombination centers on the non-passivated c-Si substrate surface is then estimated to be about 5.0×10^{11} cm^{-2}. Using the same approach, c-Si substrates with mono-layered ($R_I = 5$) and dual-layered ($R_I = 5$ and $R_C = 13$) passivation films imply dramatically decreased N_t of 4.3×10^9 cm^{-2} and 3.3×10^9 cm^{-2}, respectively. It has been reported that the dominant recombination centers on the c-Si surface consist of dangling bonds at the surface, which can be effectively passivated by the interfacial *i* a-Si:H film.[32] Based on our measurements and the corresponding calculated N_t values before and after mono-layered passivation, almost 99% of the surface recombination centers of the c-Si substrate were removed by the interfacial passivation layer.

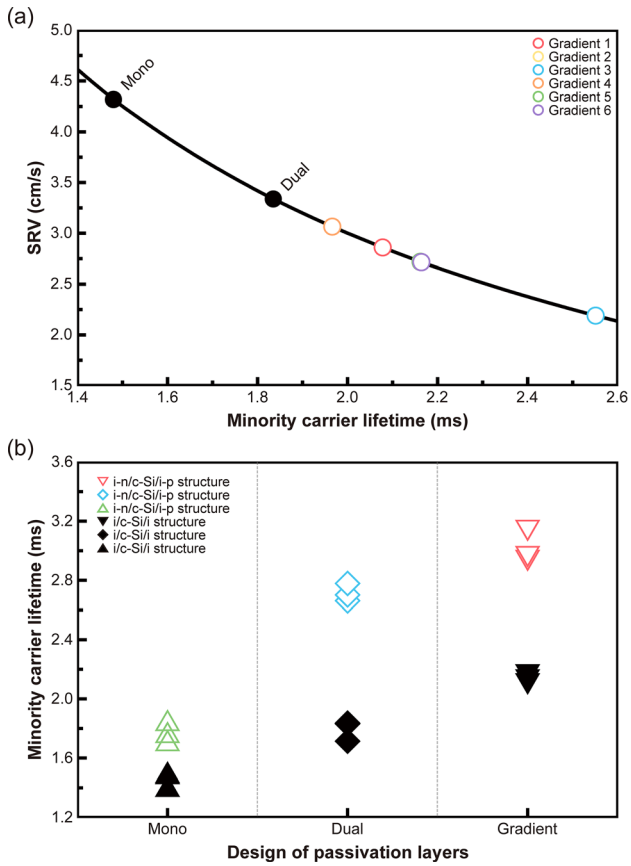

FIG. 6. (a) Calculated SRVs for c-Si substrates passivated by 10 nm i a-Si:H films for different designs of passivation layers. The black line represents the relationship between SRV and effective minority carrier lifetime, calculated by Eq. (2). (b) The effective minority carrier lifetime of the c-Si substrate passivated by 10 nm *i* a-Si:H films for different designs of passivation layers with and without 10 nm n-type and p-type a-Si:H layers on both sides.

For the gradient-layered passivation structures, determination of *N*t is complicated by the dependence of the *i* a-Si:H band gap and band-edge energies (e.g., relative to those of c-Si) on total hydrogen content (C_H), which is itself influenced by R. It has been reported that the band gap of *i* a-Si:H film changes from 1.7 eV to 2.2 eV as C_H in the film varies.[33,34] Specifically, *i* a-Si:H films deposited with low R have higher C_H and larger band gaps compared to films deposited with high R. Therefore, the interfacial *i* a-Si:H layer which was deposited with $R_I = 5$ is expected to have a larger band gap than the capping *i* a-Si:H layer with $R_C = 13$. Because the *i* a-Si:H layer with lowest R, and therefore the largest bandgap, is at the interface with the c-Si substrate, minority carrier accumulation is most likely to occur primarily at the c-Si/a-Si:H interface rather than within the *i* a-Si:H passivation layer structure. The reduction in minority carrier recombination observed experimentally in the gradient-layered passivation schemes could then occur via a reduction in trap density within the *i* a-Si:H layer, or changes in the spatial distribution and/or energy of traps in the gradient-layered structure compared to those in the dual-layered passivation films. In either case, the improvement in S_{eff} with increasing t_T is substantial. As shown in Fig. 6(a), the calculated S_{eff} values for passivation designs of Gradient 1, 2, and 3 decreased from 2.86 cm s^{-1} to 2.19 cm s^{-1} as t_T increased from 2 nm to 6 nm.

Finally, to assess the potential effect of the gradient-layered *i* a-Si:H passivation film on SHJ solar cell structures, 10 nm doped a-Si:H layers were additionally deposited on passivated c-Si using RPCVD to form an n-type a-Si:H/*i* a-Si:H/c-Si/*i* a-Si:H/p-type a-Si:H (*i*-*n*/c-Si/*i*-*p*) structure and the resulting minority carrier lifetimes were measured. Figure 6(b) shows the measured minority carrier lifetimes of c-Si substrates passivated by different passivation schemes with and without doping layers. For every passivation scheme, the measured minority carrier lifetime increased after deposition of doped a-Si:H films. The doped a-Si:H layers generate electrical field across the c-Si, so that the *i*-*n*/c-Si/*i*-*p* structure can passivate the c-Si substrate more efficiently by not only chemical passivation but also electrical passivation. Even after adding doped a-Si:H layers, *i*-*n*/c-Si/*i*-*p* structured c-Si substrate exhibited the best passivation quality, with a minority carrier lifetime of 3200 μs. Based on these results, it can be expected that the gradient-layered *i* a-Si:H passivation can improve passivation quality for the c-Si substrate and thus enhance SHJ solar cell performance.

IV. CONCLUSIONS

In summary, we have demonstrated and analyzed gradient-layered *i* a-Si:H passivation films for enhancing the passivation quality of c-Si surfaces and consequently the efficiency of SHJ solar cells. The gradient-layered passivation was obtained by depositing *i* a-Si:H films on c-Si substrates using RPCVD with interfacial, transition, and capping layers for which the H_2 to SiH_4 dilution ratios R are varied during deposition. For the interfacial and capping layer, *i* a-Si:H films were deposited with optimized R_I and R_C values, and for the transition layer, R was gradually increased from R_I to R_C during deposition. Compared to abrupt interfaces formed in dual-layered passivation, the gradual change in R in the gradient-layered passivation enables grading of the interface regions between the interfacial and capping layers. According to the measured minority carrier lifetimes of the passivated c-Si substrates, the gradient-layered *i* a-Si:H films yielded the highest passivation quality on c-Si surfaces. There was an increase in the minority carrier lifetime for c-Si substrates with gradient-layered passivation up to 2550 μs, which was higher than with mono- and dual-layered passivation schemes. After depositing doped a-Si:H layers, the *i*-*n*/c-Si/*i*-*p* structured c-Si substrate with the gradient-layered passivation scheme also showed the highest minority carrier lifetime of 3200 μs. These results suggest that the gradient-layered *i* a-Si:H film can provide high quality passivation of c-Si surfaces for a broad range of c-Si solar cell structures.

ACKNOWLEDGMENTS

Part of this work was supported by the U.S. Army Research Laboratory (monitored by Dr. Kimberly Sablon). This work was performed in part at the University of Texas Microelectronics Research Center, a member of the National Nanotechnology Coordinated Infrastructure (NNCI), which is supported by the National Science Foundation (Grant No. ECCS-1542159).

[1]E. Franklin, K. Fong, K. McIntosh, A. Fell, A. Blakers, T. Kho, D. Walter, D. Wang, N. Zin, M. Stocks, E.-C. Wang, N. Grant, Y. Wan, Y. Yang, X. Zhang, Z. Feng, and P. J. Verlinden, Prog. Photovoltaics: Res. Appl. **24**(4), 411–427 (2016).
[2]M. Lu, U. Das, S. Bowden, S. Hegedus, and R. Birkmire, Prog. Photovoltaics: Res. Appl. **19**(3), 326–338 (2011).
[3]M. A. Green, K. Emery, Y. Hishikawa, W. Warta, and E. D. Dunlop, Prog. Photovoltaics: Res. Appl. **23**(1), 1–9 (2015).
[4]M. Taguchi, K. Kawamoto, S. Tsuge, T. Baba, H. Sakata, M. Morizane, K. Uchihashi, N. Nakamura, S. Kiyama, and O. Oota, Prog. Photovoltaics: Res. Appl. **8**(5), 503–513 (2000).
[5]F. Kersten, A. Schmid, S. Bordihn, J. W. Müller, and J. Heitmann, Energy Proc. **38**, 843–848 (2013).
[6]C.-H. Lee, B.-J. Kim, and M. Shin, Prog. Photovoltaics: Res. Appl. **22**(3), 362–370 (2014).
[7]D. Deligiannis, R. Vasudevan, A. H. M. Smets, R. A. C. M. M. van Swaaij, and M. Zeman, AIP Adv. **5**(9), 097165 (2015).
[8]A. G. Aberle and R. Hezel, Prog. Photovoltaics: Res. Appl. **5**(1), 29–50 (1997).
[9]E. U. Onyegam, D. Sarkar, M. M. Hilali, S. Saha, L. Mathew, R. A. Rao, R. S. Smith, D. Xu, D. Jawarani, R. Garcia, M. Ainom, and S. K. Banerjee, Appl. Phys. Lett. **104**(15), 153902 (2014).
[10]A. H. Mahan, J. Carapella, B. P. Nelson, R. S. Crandall, and I. Balberg, J. Appl. Phys. **69**(9), 6728–6730 (1991).
[11]A. H. Mahan, J. Yang, S. Guha, and D. L. Williamson, Phys. Rev. B **61**(3), 1677–1680 (2000).
[12]J. Koh, Y. Lee, H. Fujiwara, C. R. Wronski, and R. W. Collins, Appl. Phys. Lett. **73**(11), 1526–1528 (1998).
[13]A. M. Funde, N. A. Bakr, D. K. Kamble, R. R. Hawaldar, D. P. Amalnerkar, and S. R. Jadkar, Sol. Energy Mater. Sol. Cells **92**(10), 1217–1223 (2008).
[14]J. Hu, H. M. Branz, R. S. Crandall, S. Ward, and Q. Wang, Thin Solid Films **430**(1–2), 249–252 (2003).
[15]R. García-Hernansanz, E. García-Hemme, D. Montero, A. d. Prado, J. Olea, E. Andrés, I. Mártil, and G. González-Díaz, IEEE J. Photovoltaics **6**(5), 1059–1064 (2016).
[16]K.-S. Lee, C. B. Yeon, S. J. Yun, K. H. Jung, and J. W. Lim, ECS Solid State Lett. **3**(3), P33–P36 (2014).
[17]J. Ge, Z. P. Ling, J. Wong, T. Mueller, and A. G. Aberle, Energy Proc. **15**, 107–117 (2012).
[18]H. Meddeb, T. Bearda, Y. Abdelraheem, H. Ezzaouia, I. Gordon, J. Szlufcik, and J. Poortmans, J. Phys. D: Appl. Phys. **48**(41), 415301 (2015).
[19]S. Y. Herasimenka, W. J. Dauksher, and S. G. Bowden, Appl. Phys. Lett. **103**(5), 053511 (2013).
[20]C. R. Wronski and R. W. Collins, Sol. Energy **77**(6), 877–885 (2004).
[21]J. K. Kim, S. J. Yun, J. W. Lim, and S. H. Lee, J. Electrochem. Soc. **158**(7), D430–D434 (2011).
[22]T. Kamei, P. Stradins, and A. Matsuda, Appl. Phys. Lett. **74**(12), 1707–1709 (1999).
[23]S. Hamad, G. K. Podagatlapalli, V. S. Vendamani, S. V. S. Nageswara Rao, A. P. Pathak, S. P. Tewari, and S. Venugopal Rao, J. Phys. Chem. C **118**(13), 7139–7151 (2014).
[24]G. Rajeswaran, F. J. Kampas, P. E. Vanier, R. L. Sabatini, and J. Tafto, Appl. Phys. Lett. **43**(11), 1045–1047 (1983).
[25]K. T. Butler, J. H. Harding, M. P. W. E. Lamers, and A. W. Weeber, J. Appl. Phys. **112**(9), 094303 (2012).
[26]L. Korte and M. Schmidt, J. Appl. Phys. **109**(6), 063714 (2011).
[27]X. Cheng, E. S. Marstein, H. Haug, and M. Di Sabatino, Energy Proc. **92**, 347–352 (2016).
[28]B. Pardia, G. Lim, J. Choi, S. Palei, and K. Kim, Sol. Energy **122**, 486–496 (2015).
[29]J. Oh, H.-C. Yuan, and H. M. Branz, Nat. Nanotechnol. **7**(11), 743–748 (2012).
[30]E. Yablonovitch, D. L. Allara, C. C. Chang, T. Gmitter, and T. B. Bright, Phys. Rev. Lett. **57**(2), 249–252 (1986).
[31]S. Avasthi, Y. Qi, G. K. Vertelov, J. Schwartz, A. Kahn, and J. C. Sturm, Appl. Phys. Lett. **96**(22), 222109 (2010).
[32]Z. Shu, U. Das, J. Allen, R. Birkmire, and S. Hegedus, Prog. Photovoltaics: Res. Appl. **23**(1), 78–93 (2015).
[33]K. Fukutani, M. Kanbe, W. Futako, B. Kaplan, T. Kamiya, C. M. Fortmann, and I. Shimizu, J. Non-Cryst. Solids **227–230**, 63–67 (1998).
[34]P. Gogoi, P. N. Dixit, and P. Agarwal, Pramana J. Phys. **70**(2), 351–358 (2008).